



## **A Numerical Analysis of Gas Enthalpy - Radiation Converter (GERC) by Using Single Cordierite Open-cellular Porous Plate**

Preecha Khantikomol<sup>1\*</sup> and Wasan Srimuang<sup>1</sup>

<sup>1</sup> Department of Mechanical Engineering, Faculty of Engineering and Architecture,  
Rajamangala University, Nakhon Ratchasima, Thailand 3000

\*Corresponding Author: preecha@rmuti.ac.th, (+66)80 470 5287, Fax. 044 233 074

### **Abstract**

The gas enthalpy-radiation conversion (GERC) utilizing cordierite porous material, which is a ceramic open-cellular porous material, is theoretically investigated. The mathematical model of the GERC consists of separated energy equations for fluid and solid phases, which include all modes of heat transfer i.e. conduction, convection and radiation heat transfer. The convective heat transfer between the two phases based on an empirical volumetric heat transfer coefficient proposed by Kamiuto and San San Yee is estimated. The Kamiuto radiative property model is used for the cordierite open-cellular porous material. The  $P_1$  approximation method is employed to evaluate the radiative transfer equation. While explicit finite different method is used to estimate the energy equations. The results show that the gas temperature drop across the cordierite porous converter and the gas enthalpy to thermal radiation conversion efficiency increases with the porous' thickness and is asymptotic to a certain value. Low pore per inch (*PPI*) is significantly effective to raise the asymptotic temperature drop; however it effects to decrease backward radiative heat flux.

**Keywords:** GERC, cordierite, temperature drop, pure reflective, porous converter

### **1. Introduction**

Radiative processes within open-cellular porous are fundamentally important in many high temperature system applications currently envisioned for these materials. It means that the radiative transfer becomes the dominate mode of heat transfer at high temperature [1]. Engineering applications, for example, are combustion burner [2], heat exchangers for high temperature applications [3], solar collectors, regenerators and recuperators, insulation system

[4, 5, 6, 7], manufacturing and materials processing, and proposed energy storage and conversion methods. The concept of porous and cellular metals first emerged in the beginning of the 1970s [8, 9]. High-temperature exhaust gas normally passed through an open-cellular porous material, the enthalpy of gas will be converted to radiation followed by returning to the upstream region. The exhaust gas temperature dropped significantly across the porous plate is revealed by Echigo [4]. Wang, K.Y. and Tien, C.L. [7]

established a concept of thermal insulation in flow systems, which is an application success of Echigo's work [4] for improvement of energy efficiency with the aid of consideration of scattering from the porous plates. Khantikomol et al. [10] reported that the upstream radiation temperature strongly governed the quantity of the gas temperature drop across the converter, and found that the porous plate only played an important role in a gas enthalpy-radiation converter when the equivalent black body radiation temperature coming from the upstream region  $T_{bu}$  was lower than the inlet gas temperature  $T_0$ . In addition, Khantikomol et al. [11] showed that lowering the surface reflectivity of the solid phase of a porous converter was quite effective to raise the gas temperature drop. They also measured the  $T_{bu}$  and found that the  $T_{bu}$  was independent on the mass flow rate and always was lower than the inlet gas temperature.

In the present study we make use of the cubic lattice model for the thermal and radiative properties [12] in order to theoretically investigate the thermal energy characteristic through a plane-parallel, open-cellular porous plate. In the analysis, the energy equation is solved numerically by a finite different method and the equation of transfer is solved using the  $P_1$  approximation. Three kinds of cordierite open-cellular porous are examined.

## 2. Physical model and governing equations

The physical model and coordinate system considered here are represented in Fig. 1. The following assumptions are introduced for the present analysis: 1) A high-temperature air is normally passing through an open-cellular

porous plate of a geometrical thickness  $x_0$ , the porosity  $\phi$  and the nominal cell diameter  $D_n$ , and flow-line of the system is considered in one-dimension; 2) The mass flow rate  $\rho_f u_f$  is constant everywhere; 3) Conduction through the fluid and solid phases is taken into account; 4) The fluid is transparent to all radiation, while the porous plate can emit, absorb and anisotropically scatter thermal radiation; 5) The external radiation is coming from the upstream and downstream regions of the porous plate and their intensities can be quantitatively represented using equivalent blackbody temperatures; 6) The radiative properties of the porous plate are considered to be gray; 7) The thermal and radiative properties of the gas (fluid) and porous plates depend only on the temperature. Under these assumptions, the law of conservation of energy for each phase yields the following expressions:

$$\rho_f u_f C_{pf} \frac{dT_f}{dx} = -h_v (T_f - T_s) + \phi \frac{d}{dx} \left( k_f \frac{T_f}{dx} \right), \quad (1)$$

$$f(1-\phi) \frac{d}{dx} \left( k_s \frac{dT_s}{dx} \right) + h_v (T_f - T_s) - \text{div} \mathbf{q}_R = 0, \quad (2)$$

$$\text{div} \mathbf{q}_R = \beta^* (1 - \omega^*) (4\sigma T_s^4 - G). \quad (3)$$

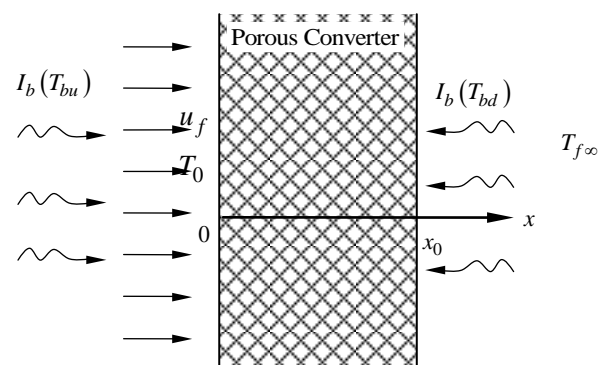


Fig. 1 The physical model and coordinate system

The associated boundary conditions for Eqs. (1) and (2) are

$$\left. \begin{aligned} x=0 & : T_f = T_{f0}, \frac{dT_s}{dx} = 0, \\ x=x_0 & : \frac{dT_f}{dx} = \frac{dT_s}{dx} = 0. \end{aligned} \right\} \quad (4)$$

$G$  and  $q_{Rx}$  appearing in Eq. (3) are the incident radiation and the net radiative heat flux, respectively, that can be determined from the equation of transfer, RTE. In the current study, the  $P_1$  approximation method is adopted to evaluate  $G$  and  $q_{Rx}$ , which has been successfully employed in previous studies [13, 14, 15]. The  $P_1$  equations are rewritten as

$$\frac{dq_{Rx}}{dx} + (1 - \omega^*) \beta^* (G - 4\sigma T_s^4) = 0, \quad (5)$$

$$\frac{dG}{dx} + 3(1 - \omega^* g^*) \beta^* q_{Rx} = 0. \quad (6)$$

The boundary conditions for Eqs. (5) and (6) are given by Marshak's ones [16]:

$$\left. \begin{aligned} x=0 & : G + 2q_{Rx} = 4\sigma T_{bu}^4, \\ x=x_0 & : G - 2q_{Rx} = 4\sigma T_{bd}^4. \end{aligned} \right\} \quad (7)$$

The  $T_{bu}$  and  $T_{bd}$  appearing in Eq. (7) is the equivalent black body radiation coming from the upstream and downstream region, respectively. The  $T_{bu}$  has been measured by Khantikomol et al. [10] that is represented as

$$T_{bu} = 0.827T_0 + 55.501 \text{ (K)}. \quad (8)$$

The forward radiative heat flux  $q_{Rx}^+$  and the backward radiative heat flux  $q_{Rx}^-$  are obtained to explain the phenomena of local radiative equilibrium throughout the open-cellular porous emitted from an infinitesimal position to

the vicinity position. These quantities are evaluated following expression:

$$q_{Rx}^+(x) = \frac{1}{2} \int_0^1 [G(x) + 3\mu q_{Rx}(x)] \mu d\mu, \quad (9)$$

$$q_{Rx}^-(x) = \frac{1}{2} \int_0^1 [G(x) - 3\mu q_{Rx}(x)] \mu d\mu. \quad (10)$$

To quantitatively evaluate the efficiency of the gas enthalpy-radiation conversion processes, the following quantity defined by a ratio of recaptured radiation to incoming energy is introduced in accordance with Wang et al. [7]:

$$\eta_c = \frac{q_{Rx}^-(0)}{\rho_f u_f C_{pm} (T_0 - T_{f\infty}) + \sigma T_{bu}^4 + \sigma T_{bd}^4}. \quad (11)$$

Here,  $C_{pm}$  is the mean specific heat capacity of fluid over a temperature range from  $T_{f\infty}$  to  $T_0$

### 3. Physical Properties

The volumetric heat transfer coefficient between the fluid and solid phases  $h_v$  was estimated using the correlation developed by Kamiuto and San San Yee [17]:

$$Nu_p = \frac{h_v D_p^2}{k_f} = 0.124 (Re_p Pr)^{0.792}, \quad (12)$$

where  $D_p$  is an equivalent strut diameter defined by

$$D_p = 2wD_n / \sqrt{\pi}. \quad (13)$$

Here,  $w$  is the dimensionless width of struts consisting of a cubic unit cell assumed in

Dul'nev's model [18] for an open-cellular porous material and is given by

$$w = 0.5 + \cos \left[ \frac{1}{3} \cos^{-1} (2\phi - 1) + \frac{4\pi}{3} \right]. \quad (14)$$

Moreover, on the basis of Dul'nev's cubic unit cell model, analytical expressions for the radiative properties of an open-cellular porous material have been developed by Kamiuto [12] and are represented as follows:

$$\left. \begin{aligned} \beta^* &= \frac{\pi}{4D_n(1-w)} \left[ (6/\pi)^{2/3} w^2 + 4w(1-w)/\sqrt{\pi} \right], \\ \omega^* &= \rho_H, \quad \tilde{g}^* = -\frac{4}{9}. \end{aligned} \right\} (15)$$

Where  $\beta^*$  denotes the scaled extinction coefficient ( $m^{-1}$ ),  $\omega^*$  denotes scaled albedo and  $\rho_H$  denotes the hemispherical reflectivity of the surface of struts and strut junctures, which is obtained by experiment. The  $\rho_H$  of cordierite is represented as follow [19, 20]:

$$\rho_H = 0.698 + 0.26\gamma. \quad (16)$$

The thermal conductivity of cordierite was taken from the data book compiled by Touloukian et al. [20] and was given as

$$k_s = 2.29 - 0.21\gamma. \quad (17)$$

Here,  $\gamma$  is defined by  $T/1000$  (K).

The physical characteristics of the examined open-cellular porous materials [21] which were used in the present study are listed on the Table 1.

**Table 1.** Physical characteristics of the examined open-cellular porous materials.

Materials	Porosity, $\phi$	PPI	$\beta^*$
Cordierite#6	0.873	6	111.64
Cordierite#13	0.870	13	245.67
Cordierite#20	0.875	20	368.25

#### 4. Numerical Analysis

For the convenience of numerical analysis, the governing equations and associated boundary conditions are rewritten in dimensionless form by introducing the following quantities:

$$\left. \begin{aligned} C_p^* &= C_p / C_{p\infty}, \quad C_{pm}^* = C_{pm} / C_{p\infty}, \\ N_R &= k_{f\infty} / 4\sigma T_{f\infty}^3 x_0, \\ Nu_p &= h_v D_p^2 / k_{f\infty}, \quad Pr = \mu_{f\infty} c_{p\infty} / k_{f\infty}, \\ Re_p &= \rho_f u D_p / \mu_{f\infty}, \\ \theta_f &= T_f / T_{f\infty}, \quad \theta_s = T_s / T_{f\infty}, \\ \xi &= x / x_0, \quad \tau_0^* = \beta^* x_0, \\ \chi &= G / \sigma T_{f\infty}^4, \quad \psi = q_{Rx} / \sigma T_{f\infty}^4. \end{aligned} \right\} (18)$$

The dimensionless forms of governing equations were solved numerically using an implicit finite difference formula. Each porous region was divided into 200 equally spaced increments for computations of  $\theta_f$  and  $\theta_s$ , whereas the optical thickness was divided into 400 equally spaced increments and the  $P_1$  equations for  $\chi$  and  $\psi$  were discretized at staggered lattice points [15].

#### 5. Results and Discussion

To examine the adequacy of numerical model in predicting the temperature profiles and

heat transfer characteristics in cordierite ( $2\text{MgO} \cdot 2\text{Al}_2\text{O}_3 \cdot 5\text{SiO}_2$ ) open-cellular porous materials, the numerical computations were made under conditions corresponding to the conversion of gas enthalpy to thermal radiation reported by Khantikomol et al. [10] and the ambient temperature ( $T_{f\infty}$ ) was assumed to be constant as 300 K. The obtained results are summarized in Figs. 2 to 6.

### 5.1 Temperature Profiles and Radiative Heat Fluxes

Figure 2 shows the temperature profiles within the 0.02m thickness of cordierite porous converter based on the conditions: the inlet gas temperature ( $T_0$ ) is 1000 K, the equivalent black body radiation temperature ( $T_{bu}$ ) is evaluated by Eq.(8), and the Reynolds number ( $Re_p$ ) is 0.5. Three kinds of cordierite open-cellular porous material were examined. It is seen from Fig.2 that the gas phase temperatures within the porous plate higher than those of solid phase. Both of gas and solid phase temperatures decrease along the porous thickness. This is caused by the fact that the porous media receive and transfer the energy by conduction with the solid matrix, by convection between gas and solid phase, and by emitting the thermal radiation into the vicinity leading to the difference of gas and solid phase temperatures and decreasing along the porous thickness. Moreover, the results also illustrate that the difference temperature between gas and solid phase of low *PPI* is higher than that of high *PPI* porous material.

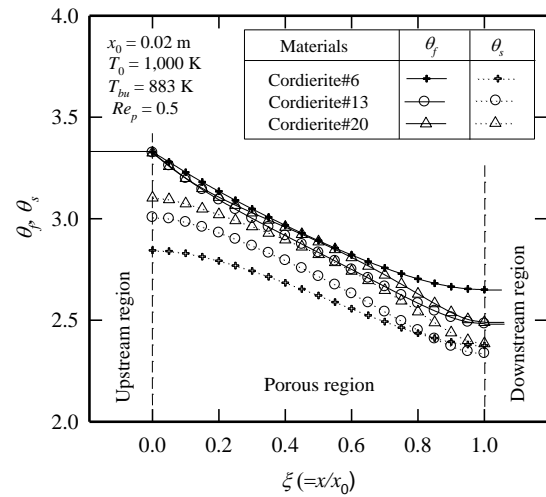


Fig. 2 Temperature profiles within the Cordierite porous converters:  $Re_p = 0.5$

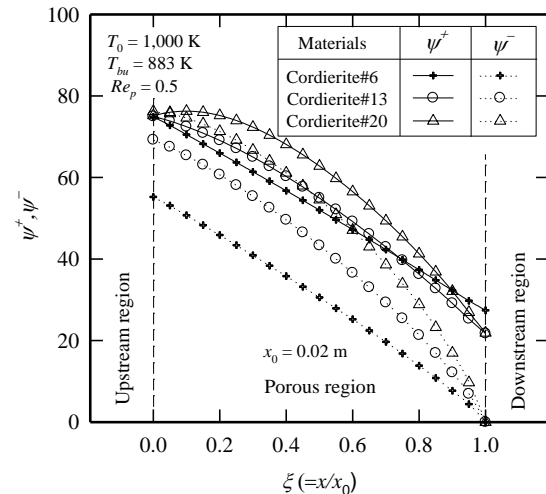


Fig. 3 Radiative heat fluxes within the Cordierite porous converters:  $Re_p = 0.5$ .

Figure 3 indicates the backward ( $\psi^-$ ) and forward ( $\psi^+$ ) radiative heat fluxes within the cordierite porous converter. The results show that the backward radiative heat flux within high *PPI* porous converter (cordierite#20) is higher than that of low *PPI* (cordierite#06), namely, high *PPI* is effective to raise the radiative heat flux. Obviously, the radiative heat fluxes quite high at the inlet of the upstream region due to the reflectivity of cordierite are rather high.

### 5.2 Effect of Thickness

From Fig.4, the gas temperature drop ( $\Delta\theta_f = (T_f(0) - T_f(x_0))/T_\infty$ ) increases with the porous thickness ( $x_0$ ) and is asymptotic to a certain limiting value  $\Delta\theta_{f\infty}$  and is well approximated by the following expression:

$$\Delta\theta_f = \Delta\theta_{f\infty} [1 - \exp(-ax_0^b)] \quad (19)$$

In Eq. (19),  $\Delta\theta_{f\infty}$ ,  $a$  and  $b$  can be obtained by using the non-linear least-square method. In the case of  $Re_p = 0.5$ , the value of  $\Delta\theta_{f\infty}$ ,  $a$  and  $b$  has been summarized in the table 2.

Table 2 Coefficients of Eq. (19) using the non-linear least-square fit ( $Re_p = 0.5$ ).

Materials	$T_0(K)$	$T_{bu}(K)$	$\Delta\theta_{f\infty}$	$a$	$b$
Cordierite#6	600	552	0.472	59.360	1.091
	800	717	0.854	57.510	1.098
	1000	883	1.240	57.560	1.109
	1200	1047	1.617	61.240	1.138
Cordierite#13	600	552	0.353	116.100	1.060
	800	717	0.712	88.050	1.026
	1000	883	1.111	74.840	1.012
	1200	1047	1.502	90.110	1.079
Cordierite#20	600	552	0.275	228.500	1.099
	800	717	0.591	161.300	1.058
	1000	883	0.962	128.600	1.040
	1200	1047	1.258	828.800	1.463

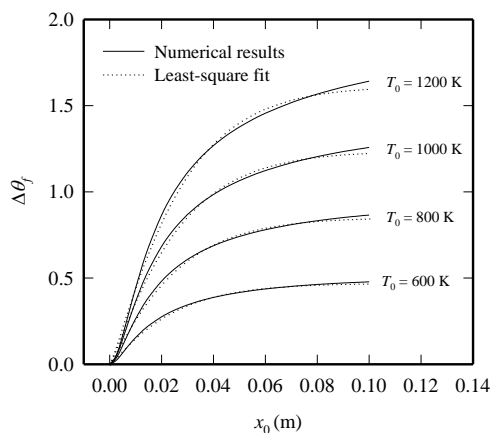


Fig. 4 Comparison between numerical results and least-squares fits of cordierite#06:  
 $Re_p = 0.5$

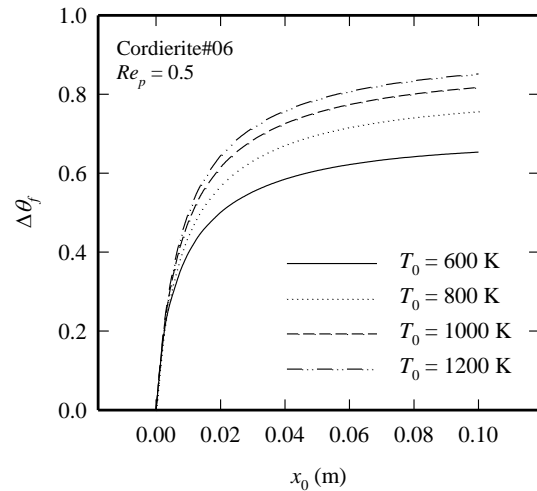


Fig. 5 Gas temperature drop across the gas enthalpy-radiation converter:  $Re_p = 0.5$

Considering Fig.4, it is seen that the gas temperature drop across the converter  $\Delta\theta_f$  increases with increasing the inlet gas temperature. That is the face that the thermal radiation plays an important role at high temperature leading to increase the backward radiation energy and increase the gas temperature drop.

Figure 5 shows the gas enthalpy to radiation conversion efficiency ( $\eta_c$ ) that was defined as Eq.(11). Obviously that it increases with the porous' thickness and is asymptotic to a certain limiting value. The conversion efficiency also increases with increasing the inlet gas temperature ( $T_0$ ).

From Figs.4 and 5, clearly that the gas porous' thickness does not effect to the gas temperature drop and the conversion efficiency at large thickness or  $x_0$  is higher than 0.04 m in the case of cordierite#06.

### 5.3 Effect of porosity and PPI

Figure 6 indicates the comparison of gas temperature drop across the three kinds of

cordierite open-cellular porous material: cordierite#06, 13 and 20. The predicted conditions were made under  $T_0 = 1000$  K and  $Re_p = 0.5$ . It is seen that the asymptotic gas temperature drop of low PPI porous converter is higher than the high PPI porous converter. It means that the low porosity and PPI are effective to raise the asymptotic gas temperature drop but are effective to decrease the radiative heat flux (as shown in Fig.3).

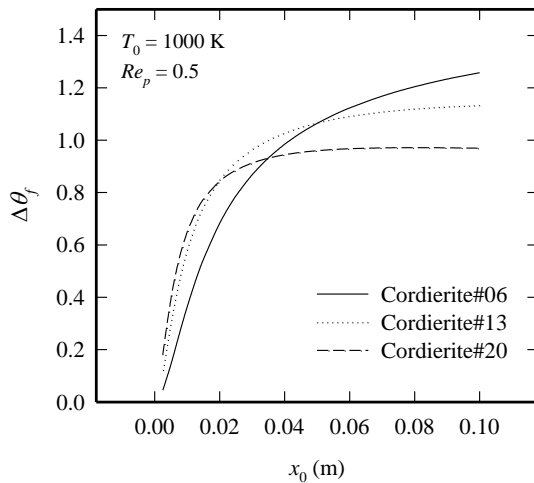


Fig. 6 Temperature drop across the cordierite porous converter:  $Re_p = 0.5$

### 5. Conclusion

The important finding of the study can be concluded that The gas temperature drop across the cordierite porous converter increase with the porous' thickness that is asymptotic to  $\Delta\theta_{f\infty}$  and can be approximated by  $\Delta\theta_f = \Delta\theta_{f\infty} [1 - \exp(-ax_0^b)]$ . Moreover, the gas enthalpy to thermal radiation conversion efficiency also increases with the porous' thickness and is asymptotic to a certain value. Low PPI porous converter is effective to increase the temperature difference between the gas and solid phase, to increase the asymptotic

gas temperature drop, and to decrease the backward radiative heat flux.

### 6. Nomenclature

$k_f$	thermal conductivity of fluid, W/(m·K)
$k_s$	thermal conductivity of porous material, W/(m·K)
$N_R$	dimensionless ratio of fluid conduction to solid radiation
$Nu_p$	Nusselt number
$Pr$	Prandtl number at inlet system
$Re_p$	Reynolds number defined by $\rho_f u_f D_p / \mu_{f\infty}$
$\chi$	dimensionless incident radiation
$\mu$	cosine of scattering angle ( $= \cos \theta$ )
$\theta_f$	dimensionless temperature of fluid phase
$\theta_s$	dimensionless temperature of solid phase
$\psi$	dimensionless net radiative heat flux
$\xi$	dimensionless coordinate in the flow direction

### 7. References

- [1] Van de Hulst, H. C.(1957). Light Scattering by Small Particles, *Dover Publications, Inc*, New York, 1957, p.103.
- [2] Weinberg, F. J. (1996). Heat-recirculating burners: principles and some recent developments, *Combust. Sci. and Tech.*, Vol. 121, pp. 3-22.
- [3] Jugjai, S. and Chuenchit, C. (2001). A Study of Energy Conversion by a Porous Combustor-Heat Exchanger with Cyclic Flow Reversal Combustion, *Int. Energy J.*, Vol. 2, No. 2, pp. 95-104.
- [4] Echigo, R. (1982). Effective Energy Conversion Method between Gas Enthalpy and



- Thermal Radiation and Application to Industrial Furnaces. *Proc.7th Int. Heat Transfer Conf.*, Vol.6, pp.361-366.
- [5] Khantikomol, P., Saito, S. and Kamiuto, K. (2008). Combined convection and radiation heat transfer in an open-cellular plate, *7th JSME-KSME Thermal and Fluids Engineering Conf.*, Sapporo Japan.
- [6] Khantikomol, P., Saito, S., and Yokomine, T. (2009). Study of Multilayer Flow Insulation utilizing Open-Cellular Porous Plates, *Proc. Int. Conf. Power Engineering (ICOPE-09)*, Vol.3, pp.37-42.
- [7] Wang, K. Y. and Tien C. L. (1984). Thermal insulation in flow system: Combined radiation and convection through a porous segment, *ASME. J. Heat Transfer.*, Vol. 106, pp. 453-459.
- [8] Barton, R.R., Carter, F. W. S., Robert, T. A., (1974). Use of reticulated metal foam as flashback arrestor elements, *Chemical Engineer - London*, Vol. 291, pp. 708-708.
- [9] Bray, H. (1972). Design opportunities with metal foam, *Engineering Materials and Design*, 1972, Vol. 16, Issue 1, pp. 19.
- [10] Khantikomol, P. and Kamiuto, K. (2008). Design Considerations of Porous Gas Enthalpy-Radiation Converters for Exhaust-Heat Recovery Systems, *J. Thermal Science and Technology*, Vol. 3 (No.2), pp. 319-329.
- [11] Khantikomol, P. and Kamiuto, K. (2008). Combined Forced-Convection and Radiation Heat Transfer in an Open-Cellular Porous Plate, *Proc. Of Int. Conf. on Thermal and Fluids Engineering (The 7th JSME-KSME)*
- [12] Kamiuto, K. (1997). Study of Dul'nev's Model for the Thermal and Radiative Properties of Open-Cellular Porous Materials, *JSME Int. J.*, Series B. 40 (1997) 577-582.
- [13] Kamiuto, K. (2000). Combined conductive and radiative heat transfer through open-cellular porous plates, *JSME Int. J.*, Series B, 2000, Vol. 43, pp. 273-278.
- [14] Kamiuto, K. (1999). Modeling of elementary transport processes and composite heat transfer in open-cellular porous materials, *Trends in Heat, Mass & Momentum Transfer*, Vol. 5, pp.141-161.
- [15] Kamiuto, K., Saito, S. and Ito, K. (1993). Numerical model for combined conductive and radiative heat transfer in annular packed beds, *Numerical Heat Transfer, Part A*, Vol. 23, pp. 433-443.
- [16] O1.Ozisik, M. N. (1973). Radiative Transfer and interactions with conduction and convection, *Jonh Wiley & Sons*, New York, USA, pp. 249-392.
- [17] Kamiuto, K. and San San Yee. (2005). Heat Transfer Correlations for Open-Cellular Porous Materials, *Int. Communi. Heat Mass Transfer*, Vol.32 (7), pp. 947-953.
- [18] Dul'nev, G.N. (1965). Heat Transfer through Solid Dispersion Systems, *Eng. Phys. J.*,Vol. 9, pp. 275-279.
- [19] Kamiuto, K. and Matsushita, T. (1998). High-temperature radiative properties of open-cellular porous materials, *Proc. 11th Int. Heat Transfer Conf.*, Vol. 7, pp. 385-390.
- [20] Touloukian, Y.S.(ed). (1967). Thermophysical Property of High Temperature Solid Materials, MacMillan, New York.
- [21] Kamiuto, K. (2008). in Cellular and Porous Materials, Willey-VCH, pp.165-198.